Check for updates

# Surface Exposure and Packing of Lipoproteins into Outer Membrane Vesicles Are Coupled Processes in *Bacteroides*

Ezequiel Valguarnera,[a] Nichollas E. Scott,[b] Philippe Azimzadeh,[a] Mario F. Feldman[a]

[a]Department of Molecular Microbiology, Washington University in Saint Louis, Saint Louis, Missouri, USA
[b]Department of Microbiology and Immunology, The University of Melbourne, Victoria, Australia

**ABSTRACT** Outer membrane vesicles (OMVs) are spherical structures derived from the outer membranes (OMs) of Gram-negative bacteria. *Bacteroides* spp. are prominent components of the human gut microbiota, and OMVs produced by these species are proposed to play key roles in gut homeostasis. OMV biogenesis in *Bacteroides* is a poorly understood process. Here, we revisited the protein composition of *Bacteroides thetaiotaomicron* OMVs by mass spectrometry. We confirmed that OMVs produced by this organism contain large quantities of glycosidases and proteases, with most of them being lipoproteins. We found that most of these OMV-enriched lipoproteins are encoded by polysaccharide utilization loci (PULs), such as the *sus* operon. We examined the subcellular locations of the components of the Sus system and found a split localization; the alpha-amylase SusG is highly enriched in OMVs, while the oligosaccharide importer SusC remains mostly in the OM. We found that all OMV-enriched lipoproteins possess a lipoprotein export sequence (LES), and we show that this signal mediates translocation of SusG from the periplasmic face of the OM toward the extracellular milieu. Mutations in the LES motif caused defects in surface exposure and recruitment of SusG into OMVs. These experiments link, for the first time, surface exposure to recruitment of proteins into OMVs. We also show that surface-exposed SusG in OMVs is active and rescues the growth of bacterial cells incapable of growing on starch as the only carbon source. Our results support the role of OMVs as "public goods" that can be utilized by other organisms with different metabolic capabilities.

**IMPORTANCE** Species from the *Bacteroides* genus are predominant members of the human gut microbiota. OMVs in *Bacteroides* have been shown to be important for the homeostasis of complex host-commensal relationships, mainly involving immune tolerance and protection from disease. OMVs carry many enzymatic activities involved in the cleavage of complex polysaccharides and have been proposed as public goods that can provide growth to other bacterial species by release of polysaccharide breakdown products into the gut lumen. This work shows that the presence of a negatively charged rich amino acid motif (LES) is required for efficient packing of the surface-exposed alpha-amylase SusG into OMVs. Our findings strongly suggest that surface exposure is coupled to packing of *Bacteroides* lipoproteins into OMVs. This is the first step in the generation of tailor-made probiotic interventions that can exploit LES-related sequences to generate *Bacteroides* strains displaying proteins of interest in OMVs.

**KEYWORDS** *Bacteroides*, OMV, hydrolases, lipoproteins, vesicles

Outer membrane vesicles (OMVs) are small spherical structures derived from the outer membranes (OMs) of most Gram-negative bacterial species. OMVs are composed of phospholipids, lipopolysaccharide (LPS), or lipooligosaccharide (LOS) and OM and periplasmic proteins (1, 2). OMVs can mediate host-microbe interactions by

facilitating long-distance delivery of virulence factors, by modulating the host immune response, and by contributing to antibiotic resistance (1, 3–8). Despite these key roles in bacterial physiology, OMV biology is poorly understood. Recent research indicates that OMVs are produced by diverse mechanisms. For example, OMVs are proposed to be generated by LPS remodeling in *Porphyromonas gingivalis*, *Salmonella enterica*, and *Pseudomonas aeruginosa* (9–12). In contrast, OMVs from *Haemophilus influenzae* and *Vibrio cholerae* are thought to be the result of an accumulation of phospholipids in the OM outer leaflet mediated by their specialized VacJ/Yrb transporter (13). Thus, it appears that there is not a universal mechanism of OMV biogenesis. For most species, including *Bacteroides* spp., OMV biogenesis remains poorly understood (5).

Species from the phylum *Bacteroidetes* compose a major part of the human gut microbiota (14, 15). OMVs from these organisms are proposed to play important roles in the commensal-host relationship, including the delivery of immunomodulatory molecules to host immune cells, an interaction that appears to help prevent colitis flare-ups in the context of inflammatory bowel disease (IBD) (7, 8). Furthermore, *Bacteroides* OMVs have been proposed to interfere with intracellular $Ca^{2+}$ signaling in host cells (16). Most studies focus primarily on two predominant species in the human gut, *Bacteroides thetaiotaomicron* and *Bacteroides fragilis*. These species produce large amounts of uniformly sized OMVs that have a protein composition distinct from that of the OM, indicating that these OMV particles are not by-products of bacterial lysis (5). Most *Bacteroides* OMV-exclusive proteins are putative acidic lipoproteins with hydrolase activity, suggesting that proteins with similar structural and physicochemical properties are selectively sorted to OMVs (5). Many *Bacteroides* enzymatic lipoproteins are encoded on polysaccharide utilization loci (PULs), which constitute ~20% of the *B. thetaiotaomicron* genome and are essential for the breakdown and acquisition of plant, fungus, and mucin complex polysaccharides (17–19). PULs typically consist of at least one TonB-dependent receptor, or SusC-like protein, and one nutrient binding accessory protein, or SusD, and they can also present other accessory proteins (20). PULs can also carry two-component systems that sense nutrient variations in the medium, with subsequent induction of polysaccharide utilization genes required for the utilization of complex carbon sources (17–19, 21–24). Hence, *Bacteroides* cells can modify the enzymatic compositions of OMVs according to available carbon sources (5). The enzymatic arsenal carried by *Bacteroides* OMVs appears to carry a "social" function, as the products of OMV-mediated hydrolysis can be utilized by other bacteria within the gut (25, 26).

Here, we further characterized the protein composition of *B. thetaiotaomicron* OMVs. We confirmed that OMVs produced by this organism contain mainly putative acidic lipoproteins with hydrolytic or carbohydrate-binding activities. Many of these OMV-enriched lipoproteins were found to be encoded by PULs. We examined the subcellular localization of the components of the archetypical PUL, the starch utilization system (Sus) (20, 27), and found that the alpha-amylase SusG and other Sus lipoproteins are highly enriched in OMVs. In contrast, the oligosaccharide importer SusC remains mostly in the OM, as previously characterized (20, 27, 28). We show that the presence of a lipoprotein export sequence (LES) mediates translocation of SusG from the periplasmic face onto the extracellular milieu and is both required and sufficient for SusG to localize preferentially to OMVs. Our results support the role of OMVs as "public goods" that can be utilized by other organisms with different metabolic capabilities.

## RESULTS

**Proteomics analysis of membrane and OMV fractions from *B. thetaiotaomicron*.** Electron micrograph analysis confirmed that *B. thetaiotaomicron* produces large amounts of uniform OMV particles (Fig. 1). We previously performed a proteomic analysis of *B. thetaiotaomicron* OMs and OMVs by employing Triton X-100 for the purification of OM proteins (5). In this work, we employed *N*-lauroylsarcosine (Sarkosyl), which has been widely used for the separation of inner membrane (IM) and OM fractions in Gram-negative bacteria (29–31) to verify that the apparent selective frac-
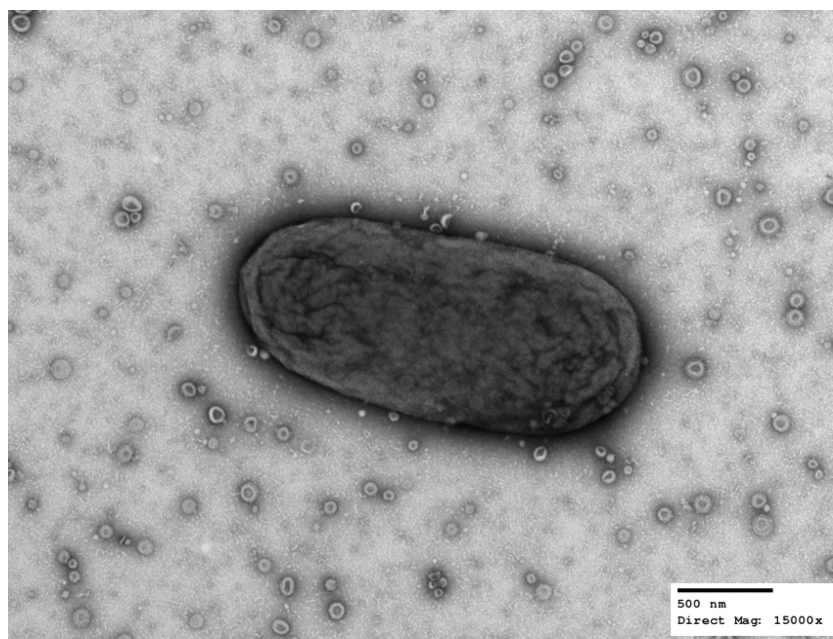
**FIG 1** *B. thetaiotaomicron* produces outer membrane vesicles (OMVs). Transmission electron microscopy of a single *B. thetaiotaomicron* cell together with OMVs in the extracellular milieu. *B. thetaiotaomicron* cells were swabbed from a solid-medium plate, suspended in PBS, and processed for TEM. Images were acquired at a direct magnification of ×15,000. The scale bar represents 500 nm. (Image courtesy of Wandy Beatty, Molecular Microbiology Imaging Facility, WUSTL.)

tionation of proteins into OM and OMV was not due to the use of a specific detergent. Using early-stationary-phase cultures from *B. thetaiotaomicron*, we prepared the different membrane fractions as indicated in Fig. S1 in the supplemental material. In our previous study, OMVs were not treated with the detergent employed to extract the IM proteins from total membrane preparations. To rule out possible detergent effects, we added an additional step consisting of incubating OMVs in 1% Sarkosyl prior to the ultracentrifugation of the samples to recover an OMV supernatant (OMV-S) and an OMV pellet (OMV-P). Samples were lyophilized for proteomic analysis by liquid chromatography-tandem mass spectrometry (LC-MS/MS), and aliquots were visualized by Coomassie blue staining (Fig. S1).

Our new data set with annotations and predicted functions and locations for proteins in all fractions is provided as Table S1 in the supplemental material. We confirmed our previous findings showing an enrichment of lipoproteins in the OMV fraction in comparison with their level in the OM fraction (Table 1; Table S2) (5). Figure 2 highlights the top enriched proteins in the OMV. We found that 18 out of the 23 OMV-exclusive lipoproteins from our previous study are also enriched in the new OMV preparations (5). We then cloned three OMV- and three OM-enriched proteins identified in our studies into the expression vector pFD340 as C-terminal 6×His-tagged proteins to confirm their localization by Western blotting. Figure 3a shows that a putative cell surface protein (BT_1488), as well as a putative calpain-like protease (BT_3960) and a putative zinc peptidase (BT_3237), is highly enriched in OMVs. Figure 3b shows that BT_0418, BT_2844, and BT_2817, identified as OM-enriched proteins by MS, are retained at the OM and are not present in OMVs. BT_0418 is a porin F ortholog (8-β-strand protein with a peptidoglycan-binding domain), BT_2817 is a TonB-dependent receptor (22-β-strand protein), and BT_2844 is a lipoprotein-containing tetratricopeptide repeat (TPR) motif. Both BT_0418 and BT_2817 are not predicted to be lipoproteins, they carry a signal peptidase I (SPI) cleavage site, and they do not contain the lipoprotein attachment cysteine residue. Before cloning this group of OMV- and OM-enriched proteins, we observed that the automated start codon annotation for

**TABLE 1** Top 20 most OMVp-enriched proteins, including protein name and enrichment value[a]

| Gene name | Protein name | log2 LFQ (OMVp/OM) |
|---|---|---|
| BT_3382 | Putative GH10/39 family protein | 13.70 |
| BT_1488 | Putative cysteine protease | 11.36 |
| BT_3960 | Putative calpain-like protease | 11.07 |
| BT_3381 | Putative GH10/39 family protein | 10.48 |
| BT_3383 | Putative GH10/39 family protein | 10.29 |
| BT_3148 | Putative adhesin | 10.12 |
| BT_2317 | Putative fimbrial protein | 9.61 |
| BT_p548229 | Putative fimbrial protein | 9.21 |
| BT_3147 | Putative adhesin | 9.18 |
| BT_1792 | Putative cell surface protein | 9.05 |
| BT_3740 | Putative cell adhesion protein | 9.02 |
| BT_3630 | Putative fimbrial protein | 8.78 |
| BT_2479 | Putative imelysin-like protein | 8.36 |
| BT_1826 | Putative GH31-like family protein | 8.29 |
| BT_3067 | Uncharacterized protein | 8.09 |
| BT_3066 | Uncharacterized protein | 7.84 |
| BT_4606 | Uncharacterized protein | 7.83 |
| BT_2658 | Putative cell adhesion protein | 7.77 |
| BT_1063 | Putative cell adhesion protein | 7.72 |
| BT_0166 | Putative thioredoxin | 7.69 |
| BT_2989 | Uncharacterized protein | 7.63 |

[a]LFQ, label-free quantification.

some open reading frames (ORFs) (BT_0418 and BT_2844) seemed incorrect. Any mistakes in start codon-predicted annotations were corrected accordingly (see Materials and Methods). These sets of experiments demonstrate that lipoproteins are indeed differentially sorted between OMs and OMVs.

**Common features of OMV-enriched lipoproteins.** Consistently with our previous results, we found that lipoproteins enriched in OMVs are acidic, with an average isoelectric point of 4.86 (5). We also determined that OMV-enriched lipoproteins possess a negatively charged rich amino acid motif, $S(D/E)_3$, adjacent to the cysteine residue required for lipoprotein attachment (Fig. 4; Table S2). A similar motif [K-(D/E)$_2$ or Q-A-(D/E)$_2$] in the oral pathogen *Capnocytophaga canimorsus*, a member of the *Bacteroidetes* phylum, has recently been described. The report showed that this motif functions as a lipoprotein export signal (LES) required for surface exposure of OM lipoproteins (32). The authors also showed that proteins carrying a LES from *B. fragilis*
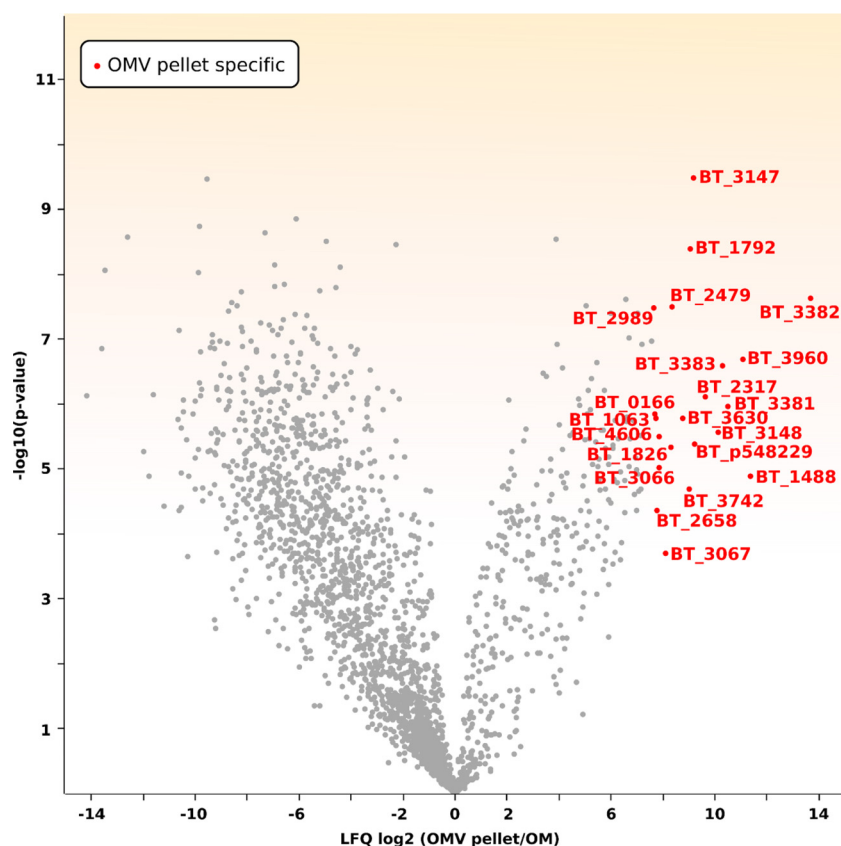
**FIG 2** The *B. thetaiotaomicron* OMV pellet (OMVp) protein content is different from that of the OM. Three hundred micrograms of each preparation and biological replicates of purified OM and OMVp proteins were digested with trypsin. The resulting peptides were enriched and then analyzed via liquid chromatography coupled to tandem mass spectrometry (LC-MS/MS) as explained in Materials and Methods, followed by protein identification with the Mascot search engine using the UniProt database. Volcano plot shows OM and OMVp protein populations. Red labels indicate the proteins with the highest OMVp enrichment in comparison to that of OM.

were exposed when expressed in *C. canimorsus*. We found that many OMV-enriched *B. thetaiotaomicron* lipoproteins are putative protein and sugar hydrolases required for the breakdown of complex nutritional sources. The presence of a LES on OMV-enriched proteins is consistent with their annotated functions, as they are required to face the extracellular milieu to access their cognate substrates. Conversely, OM-enriched lipoproteins like BT_2844 do not carry a LES motif. These proteins have lower sequence conservation and lower frequency of negatively charged amino acids along the residues adjacent to the lipoprotein attachment cysteine and are therefore expected to be oriented toward the periplasmic face of the OM (Fig. 4b; Table S2).

**SusG and other Sus lipoproteins are enriched in OMV, and SusC is retained at the OM.** In *B. thetaiotaomicron*, hydrolytic lipoproteins are encoded mainly in PULs. PUL and PUL-like operons account for approximately 20% of the *B. thetaiotaomicron* genome. Thirty-six lipoproteins encoded in PUL and PUL-like operons were found in our OMV-enriched proteins. One of the most studied lipoproteins from *B. thetaiotaomicron* is the α-amylase SusG, encoded by the *sus* operon and essential for starch catabolism (33, 34). The *sus* operon has been shown to be induced by starch and maltooligosaccharides (35). Our MS data show that even under noninducing conditions, two lipoproteins encoded by the *sus* operon, SusD and SusE, are enriched in OMVs (Table S2). Given the importance of starch in the mammalian diet, we investigated the subcellular localization of the components of the Sus operon. We found that all Sus lipoproteins, in particular SusG, are enriched in the OMV. The only exception was the porin SusC, which is retained mostly at the OM (Fig. 5). We also observed considerable levels of
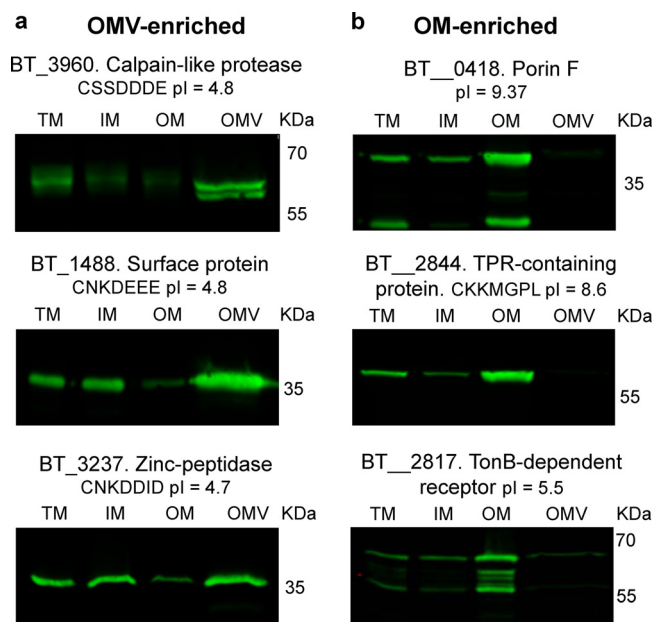
**FIG 3** Validation of OMV- and OM-enriched proteins. Candidate ORFs that encode proteins identified in our MS analysis as OMV or OM enriched were cloned into pFD340 with a C-terminal 6×His tag. Constructs were introduced into *B. thetaiotaomicron* by conjugation, generated strains were grown in TYG medium, and fractions were prepared. Ten micrograms of each fraction was subjected to 12% SDS-PAGE and analyzed by Western blotting using anti-His polyclonal antibodies. (a) OMV-enriched proteins; (b) OM-enriched proteins. The isoelectric point as well as the residues following the lipoprotein attachment cysteine (for lipoproteins) are indicated below the protein name.

SusD in the OM, concomitant with its strong functional interaction with SusC (28). This result suggests that PUL components can exert their biological effect not only at the level of the outer membrane but also through OMVs. These findings represent a localization split for the components of the *sus* operon exclusively and need to be further validated for other *sus*-like systems through the *B. thetaiotaomicron* genome, especially because we observed other SusC-like proteins enriched in both OMs and OMVs (Table S2).
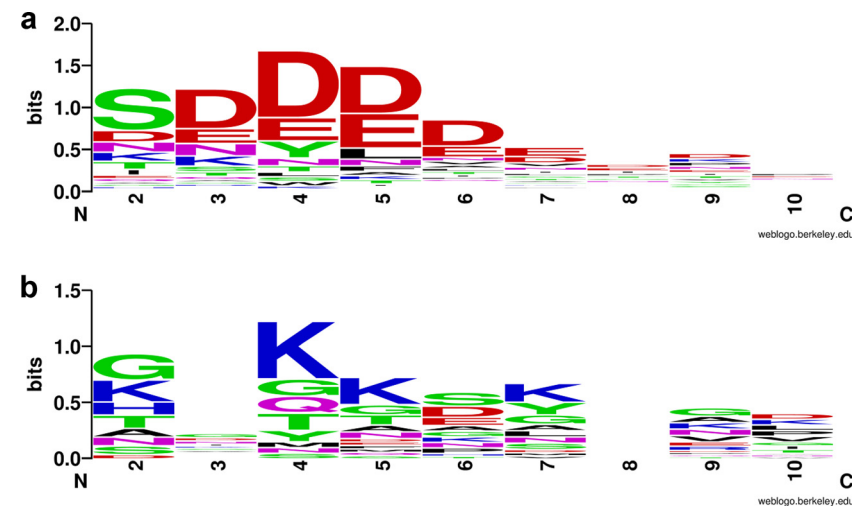


**FIG 4** OMV-enriched proteins show a conserved N-terminal LES motif. The top 91 OMV-enriched proteins (a) and top 24 OM-enriched proteins (b) were aligned using the lipoprotein attachment cysteine at the +1 position (not shown in the logo), followed by the 9 C-terminal contiguous residues. The lipoprotein export sequence (LES) consensus was generated using WebLogo (https://weblogo.berkeley.edu/logo.cgi) (56).
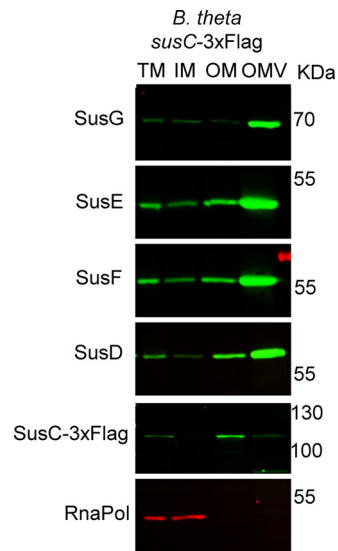
**FIG 5** Sus lipoproteins are OMV enriched, while SusC is OM enriched. *B. thetaiotaomicron* cells containing a tagged genomic copy of *susC* with a 3×Flag tag were grown in TYM medium (TYG recipe with 0.5% maltose instead of glucose for induction of the *sus* operon). Fractions were prepared and analyzed by 12% SDS-PAGE and Western blotting using specific anti-Sus, anti-Flag, and anti-RNApol antibodies.

**LES is required for SusG exposure and packing into OMVs.** All *B. thetaiotaomicron* endoglycanases involved in the first step of polysaccharide breakdown, including SusG, are surface-exposed lipoproteins (33, 36). Because all OMV-enriched lipoproteins contain a LES motif, we investigated the link between surface exposure and packing into OMVs. SusG contains only two Asp residues following the +2 Ser residue, and therefore, for the purpose of this work, we provisionally define its LES motif as CSDD. We performed a mutational analysis on the LES motif of SusG and analyzed the localization of the protein by fractionation and Western blotting (Fig. 6). We cloned wild-type (WT) His-tagged SusG and a set of SusG derivatives carrying amino acid
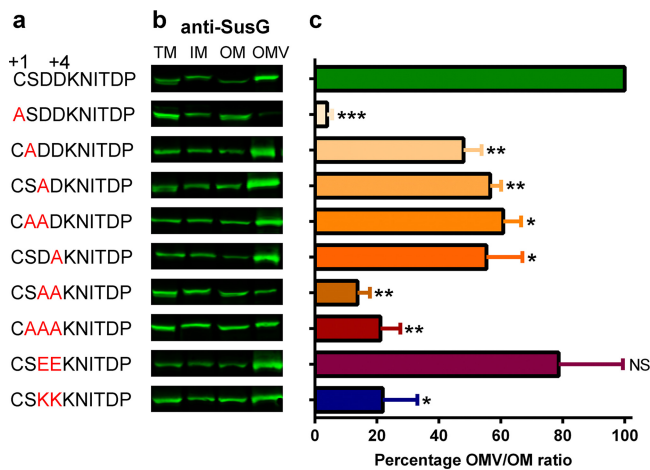


**FIG 6** SusG LES is required for efficient packing into OMVs. (a) SusG LES point mutants were generated on pFD340/*susG*-6×His using Quick site-directed mutagenesis. (b) Constructs were introduced in the ΔsusG background, and generated strains were grown in minimal medium with glucose as the only carbon source. Fractions were prepared and analyzed by SDS-PAGE and Western blotting using anti-SusG antibodies. (c) OMV/OM ratios were calculated using the fluorescence signal values for each protein and are plotted as a percentage of the WT OMV/OM ratio (100%). Statistical significance was determined by unpaired *t* test of each LES variant in comparison with values for the wild-type LES strain. *, *P* values < 0.03. NS, not significant. The experimental results are representative of those of three biological replicates; shown are mean values with standard deviations (SD) for two technical replicates.
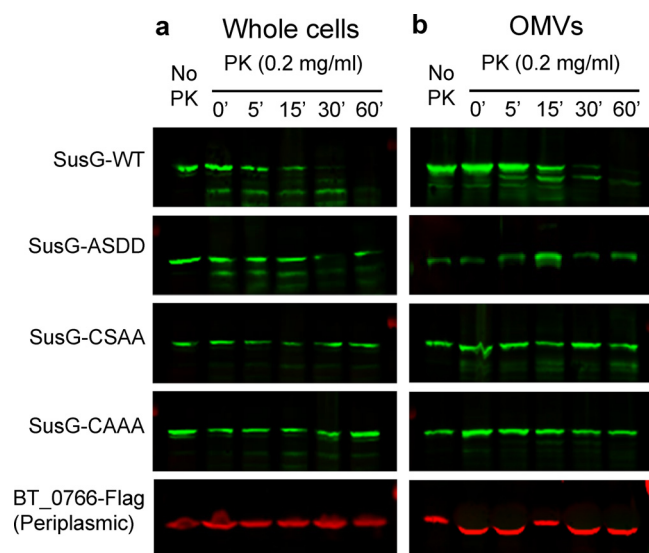
**FIG 7** The LES is required for SusG surface exposure. WT SusG and the LES mutants were assessed for their surface exposure by proteinase K assays using whole cells (a) and OMVs (b). Proteinase K (PK) was added and incubated at 37°C; at different times (in minutes), aliquots were TCA precipitated and analyzed by SDS-PAGE and Western blotting using anti-SusG antibodies. We used 3×Flag-tagged BT_0766, a periplasmic soluble protein found in OMVs, as an outer membrane and OMV integrity control.

replacements in the LES (Fig. 6a) and expressed them in the ΔsusG strain (37). Replacement of the lipid attachment site (C23) by Ala resulted in abrogation of SusG recruitment into OMVs. Furthermore, substitution of a single Asp residue with Ala (CSAD, CSDA, CAAD) decreased OMV packaging (~50% relative to that in the WT), while mutation of both Asp residues by either Ala or Lys (CSAA, CAAA, CAKK) had a more dramatic effect (~15% relative to that of the WT) (Fig. 6c). Conservative replacement of Asp by Glu (CSEE) displayed a WT-like behavior. These results indicate that the LES motif $CS(D/E)_2$ is required for SusG packaging into OMVs.

The LES motif has been defined as a surface exposure tag in *C. canimorsus* (32). We used the WT LES SusG construct as well as the non-Asp variants (CSAA, CAAA) to determine whether this motif is also required for surface exposure in *B. thetaiotaomicron*. Whole cells and OMVs from the different strains were subjected to proteinase K (ProK) sensitivity analysis. Only the WT SusG was degraded by ProK (Fig. 7). As a control, we employed a periplasmic soluble protein that localizes into the lumens of OMVs (BT_0766) and is therefore protected from ProK degradation. Taken together, these experiments confirm that LES mediates both SusG surface exposure and enrichment in OMVs.

**OMVs containing SusG rescue the ΔsusG strain's growth in starch.** Our experiments demonstrated that SusG is surface exposed and packed into OMVs. OMVs carrying certain glycosyl hydrolases can digest complex polysaccharides, providing essential nutrients to bacteria unable to degrade these substrates (25, 26). The ΔsusG strain is unable to grow on minimal media with starch as the sole carbon source (Fig. 8). We investigated whether surface exposure of OMV-delivered SusG can rescue the ΔsusG growth phenotype on starch. For this, we employed OMVs produced by the ΔsusG strain expressing WT SusG and SusG with a mutated LES (ASDD, CSAA, and CAAA). The ASDD mutation renders soluble SusG in the periplasm, while the CSAA and CAAA SusG variants face the periplasmic side of the OM (Fig. 7). Purified OMVs were added to the ΔsusG strain in minimal media containing starch. Only WT OMVs restored the growth of the ΔsusG strain to wild-type levels (Fig. 8). OMVs from the susG deletion-carrying vector control (pFD340) or expressing the nonlipoprotein mutant (ASDD) or the CSAA mutant were unable to rescue the expression of SusG, while the CAAA mutant displayed an intermediate phenotype. All together, our results indicate
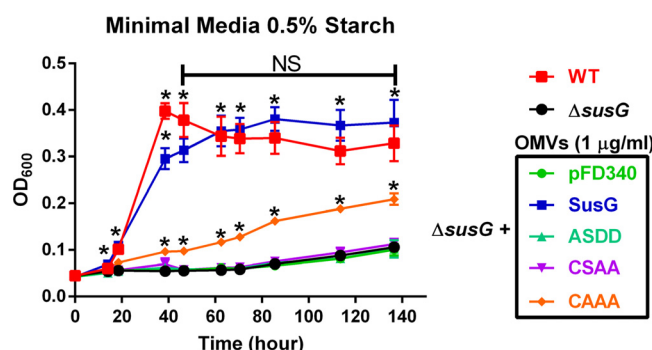
**FIG 8** OMVs displaying WT SusG can rescue a strain with a ΔsusG growth phenotype on starch as the carbon source. WT and ΔsusG strains were grown overnight in TYG medium. Cultures were washed with minimal medium without any carbon source and normalized by OD. Minimal medium with 0.5% starch as the only carbon source was inoculated with WT or ΔsusG strains to a final $OD_{600}$ of 0.05. OMVs purified from the ΔsusG strain containing different pFD340 derivatives were added to the ΔsusG cultures in minimal medium with starch (1-µg/ml final concentration of OMVs). Aliquots were taken at different times, and the $OD_{600}$ was measured to determine growth. Statistical significance when two growth curves were compared was determined by performing one pair of an unpaired *t* test analysis per each time point. *, *P* values < 0.01. The experiment is representative of three biological replicates; shown are mean values with SD for three technical replicates.

that OMVs carrying only surface-exposed SusG can mediate cross-feeding of other bacteria.

## DISCUSSION

The human gut microbiome is composed largely of species from the *Bacteroides* genus. *Bacteroides* spp. are important for gut homeostasis (14, 15). They establish ecological interactions with each other and are also involved in host-commensal relationships, especially regarding the development of the immune system (7, 8, 16). Here, we show that *B. thetaiotaomicron* produces large amounts of uniformly sized OMVs. Using an optimized methodology for the purification of different membrane fractions, we confirmed that OMVs are highly enriched with lipoproteins, particularly glycosyl hydrolases. Our MS data identified the presence of a lipoprotein exposure sequence (LES) in all OMV-enriched lipoproteins. Employing the α-amylase SusG as a model, we confirmed that the LES is required for surface exposure and showed that it also mediates recruitment into OMVs. To our knowledge, this is the first identification of coupling surface exposure to protein sorting into OMVs.

A few lipoprotein surface transport mechanisms in Gram-negative bacteria have been described (38–41). Shuttling of a group of *Neisseria meningitidis* lipoproteins to the surface is dependent on proteins Slam1 and Slam2, although the sorting mechanism has not been defined (41, 42). Moreover, the well-studied Bam system for folding of beta-barrel proteins in the outer membrane has been shown to export specific lipoproteins (39). We have not identified orthologs of Slam1 or Slam2 by sequence similarity in any *Bacteroides* genomes. The existence of LES motifs in *B. thetaiotaomicron* lipoproteins, together with the discovery of the LES in *C. canimorsus*, suggests the existence of a conserved phylum-wide mechanism that flips specific lipoproteins toward the extracellular milieu among *Bacteroidetes*. Defining a functional LES in *Bacteroides* spp. constitutes the first step toward the identification of the machinery that mediates lipoprotein surface exposure in these organisms. Our experiments confirmed that the two Asp residues in positions +3 and +4 respecting the lipid attachment site (+1) are essential components of SusG LES. The proposed *B. thetaiotaomicron* LES motif $CS(D/E)_2$ is similar but not identical to the $K-(D/E)_2$ or $Q-A-(D/E)_2$ LES proposed for *C. canimorsus*. An exhaustive mutagenesis analysis of multiple proteins from several species will be required to exactly define a consensus sequence for the LES motif among *Bacteroidetes*.

MS results show that OMV-enriched lipoproteins contain a LES motif, suggesting
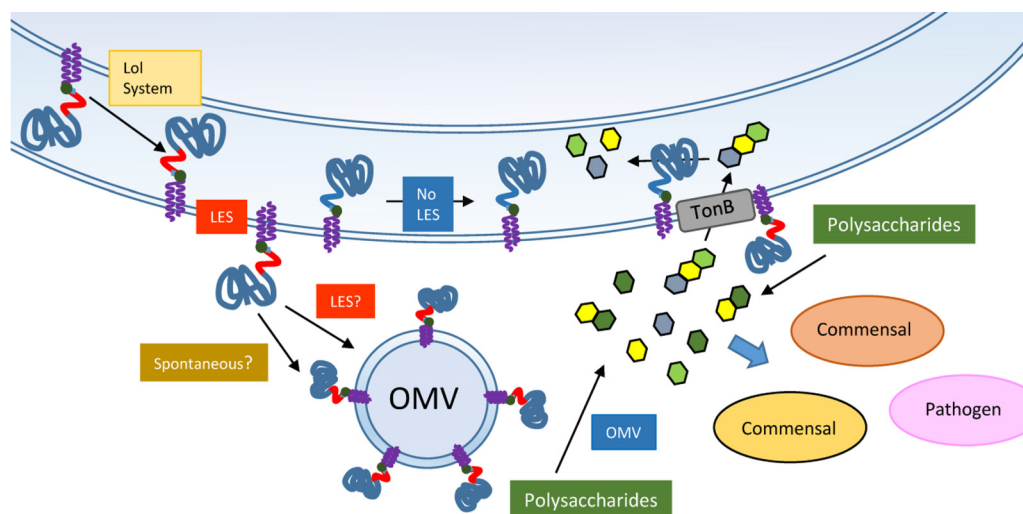
**FIG 9** A model for SusG LES-mediated surface exposure and packing into OMV. The SusG lipoprotein is probably transported to the OM by a machinery homologous to the LOL system. The presence of a LES sequence mediates the surface exposure of SusG and its incorporation into OMVs. The LES might have a dual role, where it is required for both surface exposure and OMV packing, or it might be involved only in surface exposure; biophysical properties of lipoproteins would be determinant for packing into OMVs. Surface-exposed SusG in OMVs as well as in the OM hydrolyzes starch molecules into oligosaccharides that can be imported by TonB-dependent receptors by the OMV-producing cell, as well as other commensal and pathogen organisms.

that most if not all OMV-enriched lipoproteins are surface exposed in a LES-dependent manner (Fig. 9). We can speculate with two models to account for this correlation between surface exposure and OMV recruitment of lipoproteins. One possibility is that the LES sequence is somehow recognized by a putative OMV sorting machinery, packaging them preferentially into vesicles. Alternatively, exposed lipoproteins might be recruited into OMVs based on their biophysical properties. Uncoupling surface exposure with OMV packaging is currently not possible, and future work will be required to unravel the molecular basis of the link between these two processes.

In the current models for PUL systems, the hydrolytic enzymes and the oligosaccharide importers are present at the outer membrane (20, 36). However, we determined that functional glycosyl hydrolases are packed mainly into OMVs. We also found that the glycosidases present in OMVs can provide substrates to support the growth of other bacteria, in agreement with the previously proposed function of OMVs as public goods (25, 26). We propose a model in which, in a process involving the LES, the glycosidases are sequentially surface exposed and sorted into OMVs (Fig. 9). The secreted OMVs, armed with an arsenal of hydrolases, can digest diverse dietary polysaccharides and host glycoconjugates, making the mono- and oligosaccharides available to all members of the microbiota. Depending on the diet composition, *Bacteroides* spp. can induce and package different enzyme repertoires, and therefore, members of the microbiota can act as donors or acceptors in their ecological niches. In addition, pathogens such as *Campylobacter*, *Salmonella*, and *Clostridium* can also benefit from the glycosidic activity contained in OMVs (43, 44). From an evolutionary and social standpoint, it is not clear how beneficial OMV-mediated hydrolysis is for the producing organisms. On one side, it is expected that hydrolytic OMVs make the nearby gut environment more mixed in its nutritional composition, rendering the producers more susceptible to cheating by consumers. On the other side, it is tempting to speculate that OMVs might have counteracting benefits to the producers, such as a higher efficiency of hydrolysis than that of OM-anchored enzymes (by increasing the enzymatic surface) and, potentially, an increase in the intestinal surface that could be colonized by its being able to access substrates through a longer stretch of the colonic niche.

We have identified a set of OMV- and OM-enriched proteins that may be employed

as markers to investigate the process of OMV biogenesis through the visualization of OMV in the mammalian gut. For example, these markers would allow the differentiation *in vivo* between bona fide OMV and cell lysis-derived material. Furthermore, the identification for the first time of a role for the LES as a signal for protein transport into OMVs constitutes a starting point for the design of novel probiotic interventions in animal and human health. In the future, the LES of SusG or other OMV proteins might be employed to engineer *Bacteroides* strains to secrete OMVs packed with medically relevant proteins in the mammalian gut.

## MATERIALS AND METHODS

**Bacterial strains and growth conditions.** Oligonucleotides, strains, and plasmids are described in Table S3 in the supplemental material. *Bacteroides* strains were grown in an anaerobic chamber (Coy Laboratories) using an atmosphere of 10% $H_2$, 5% $CO_2$, 85% $N_2$. For liquid growth, tryptone-yeast extract-glucose (TYG), TYM (TY medium supplemented with 0.5% maltose instead of 0.5% glucose), or minimal media supplemented with 0.5% glucose or 0.5% potato starch were prepared as previously described (17, 45). Brain heart infusion (BHI) agar with 10% defibrinated horse blood was used as a solid medium. Antibiotics were used as follows: ampicillin at 100 $\mu$g/ml, erythromycin at 25 $\mu$g/ml, and bromodeoxyuridine at 200 $\mu$g/ml.

**Construction of plasmids, mutagenesis, and generation of the *susC*-3×Flag strain.** Constructs for overexpression were built on pFD340 (46). Inserts obtained by PCR were digested with restriction enzymes, purified, and ligated onto the digested vector pFD340 as previously reported. For all 6×His-containing constructs, the tag was added to the C terminus of the ORF product by including the 6×His sequence in the reverse primer used for cloning into pFD340 (Table S3). In the cases of BT_0418 and BT_2844, we detected that the putative correct start codons extend 9 and 10 amino acids into the N terminus of the sequence, respectively, and included that information for the cloning of both genes. For cloning of BT_0766-Flag into pFD340, purified PCR inserts were integrated into PCR-amplified pFD340 using an In-Fusion cloning kit (Clontech). Mutagenesis of pFD340/*susG*-6×His was carried out by inverse PCR with *Pfu* Turbo (Agilent) using overlapping oligonucleotides carrying the mismatch required as described elsewhere. Generation of a *susC*-3xFlag strain was carried out using the *B. thetaiotaomicron* Δ*tdk* strategy as previously described (47). Briefly, 1,000-bp upstream and downstream fragments of a C-terminal *susC*-3xFlag translational fusion were cloned into pExchange-*tdk*. Constructs were conjugated into *B. thetaiotaomicron* Δ*tdk* cells using previously transformed *Escherichia coli* S17-1 λ*pir* as a donor, and strain plating and selection were performed as previously described (47).

**OMV preparations.** Outer membrane vesicles were purified by ultracentrifugation of filtered spent media as previously described by our group (5). For MS analysis, OMV preparations were resuspended in 50 mM HEPES, pH 7.4, and *N*-lauroyl sarcosine was added to a 1% final concentration in 1.5 ml polyallomer tubes (Beckman Coulter). Samples were incubated with gentle rocking for 1 h at room temperature (RT) and ultracentrifuged at 100,000 × *g* for 2 h at RT. Supernatants were recovered (OMV-S) and pellets (OMV-P) were resuspended in 50 mM HEPES, pH 7.4. Protein content was quantified using a DC protein assay kit (Bio-Rad). Fractions were lyophilized for MS analysis.

**Membrane preparations.** Total membrane preparations were performed by cell lysis and ultracentrifugation as previously described (5). For separation of the inner membrane (IM) and OM, total membranes were resuspended in 50 mM HEPES, pH 7.4, using a 2-ml glass tissue grinder with a polytetrafluoroethylene (PTFE) pestle (VWR), and *N*-lauroyl sarcosine was added to a 1% final concentration in 1.5-ml polyallomer tubes (Beckman Coulter). Samples were incubated with gentle rocking for 1 h at RT and ultracentrifuged at 100,000 × *g* for 2 h at RT. Supernatants were recovered (IM) and pellets were resuspended in 50 mM HEPES, pH 7.4. Protein content was quantified using a DC protein assay kit (Bio-Rad). Fractions were lyophilized for MS analysis.

**Mass spectrometry analysis. (i) Protein cleanup and in-solution digestion.** Lyophilized protein preparations were solubilized in lysis buffer (4% SDS, 10 mM, 100 mM Tris, pH 8.5) by boiling them for 10 min, and the protein content was assessed by the bicinchoninic acid (BCA) protein assay according to the manufacturer's instructions. Three hundred micrograms of each preparation and biological replicate was adjusted to a volume of 200 $\mu$l and precipitated overnight using 800 $\mu$l of ice-cold acetone (1:4, vol/vol). Samples were spun down at 16,000 × *g* for 10 min at 0°C to the resulting protein precipitate, and acetone was removed. Residue acetone was driven off at 70°C for 5 min. Protein precipitants were resuspended in 6 M urea, 2 M thiourea, 40 mM $NH_4HCO_3$ and reduced/alkylated prior to digestion with Lys-C (1/200, wt/wt) and then trypsin (1/50, wt/wt) overnight as previously described (48). Digested samples were acidified to a final concentration of 0.5% formic acid and desalted with using $C_{18}$ stage tips (49, 50).

**Label-free quantification (LFQ)-based quantitative proteomic LC-MS.** Prepared purified peptides were resuspended in buffer A* (2% acetonitrile, 0.01% trifluoroacetic acid) and separated using a two-column chromatography setup composed of a PepMap100 $C_{18}$ 20-mm by 75-$\mu$m trap column and a PepMap $C_{18}$ 500-mm by 75-$\mu$m analytical column (ThermoFisher Scientific). Samples were concentrated onto the trap column at 5 $\mu$l/min for 5 min and infused into an Orbitrap Q-Exactive Plus mass spectrometer (ThermoFisher Scientific) at 300 nl/min via the analytical column using a Dionex Ultimate 3,000 ultrahigh-performance liquid chromatograph (UPLC) (ThermoFisher Scientific). One-hundred-twenty-five-minute gradients were run, altering the buffer composition from 1% buffer B to 28% buffer B over 95 min, from 28% buffer B to 40% buffer B over 10 min, and then from 40% buffer B to 100% buffer

B over 2 min; the composition was held at 100% buffer B for 3 min and then dropped to 3% buffer B over 5 min and held at 3% buffer B for another 10 min. The Q-Exactive mass spectrometer was operated in a data-dependent mode, automatically switching between the acquisition of a single Orbitrap MS scan (60,000 resolution) and 15 MS-MS scans (Orbitrap HCD; 35,000 resolution; maximum fill time, 110 ms; and AGC [automatic gain control] at $2 \times 10^5$).

**Mass spectrometry data analysis.** Identification and LFQ analysis were accomplished using Max-Quant (v1.5.3.1) (51). Searches were performed against the *B. thetaiotaomicron* (strain ATCC 29148/VPI-5482) proteome (UniProt proteome identifier UP000001414, downloaded 20 May 2017, 4,782 entries) with carbamidomethylation of cysteine set as a fixed modification and with variable modifications of oxidation of methionine and acetylation of protein N termini. Searches were performed with trypsin cleavage specificity allowing 2 miscleavage events, with a maximum false discovery rate (FDR) of 1.0% set for protein and peptide identifications. To enhance the identification of peptides between samples, the Match Between Runs option was enabled with a precursor match window set to 2 min and an alignment window of 10 min. For label-free quantitation, the MaxLFQ option within MaxQuant (52) was enabled in addition to the requantification module. The resulting protein group output was processed within the Perseus (v1.4.0.6) (53) analysis environment to remove reverse matches and common protein contaminates prior. For LFQ comparisons, missing values were imputed using Perseus. Visualization was done using Perseus and R. Predicted localization and topology analysis for proteins identified by MS was performed using LipoP and TOPCONS (54, 55).

**SDS-PAGE and OMV/OM ratio determination.** Membrane and OMV fractions were analyzed by standard 10 to 12% Tris-glycine SDS-PAGE, as described elsewhere. Briefly, 10 $\mu$g of each fraction (transmembrane [TM]/IM/OM/OMV) was loaded onto an SDS-PAGE gel and transferred onto a nitrocellulose membrane, and Western blotting was performed using the LI-COR system. Membranes were blocked using Tris-buffered saline (TBS)-based Odyssey blocking solution (LI-COR). Primary antibodies used in this study were rabbit polyclonal anti-His (ThermoFisher), mouse monoclonal anti-Flag M2 (Sigma), mouse monoclonal anti-*E. coli* RNApol subunit alpha (Biolegend), and mouse polyclonal anti-SusD/E/F/G (Nicole Koropatkin/Eric Martens, University of Michigan). Secondary antibodies used were IRDye anti-rabbit 780 and IRDye anti-mouse 680 antibodies (LI-COR). Imaging was performed using an Odyssey CLx scanner (LI-COR).

For validation of MS data, duplicate SDS-PAGE gels were stained with Coomassie blue as described elsewhere, and gel images were acquired to determine fraction quality and relative abundance (Fig. S2 and S3). For OMV/OM determination of SusG-6×His experiments, cells were grown in minimal medium with glucose and fractions were prepared as described previously for OMV and membrane preparations in this section. After transference of the preparations to SDS-PAGE gels, nitrocellulose membranes were incubated with Revert total protein stain as described by the manufacturer (LI-COR) and imaged immediately at 680 nm (Fig. S4). After the imaging, Western blotting using SusG antibodies was carried out and membranes were scanned at 780 nm. Total intensity values were calculated for each lane using the Odyssey scanner software (Image Studio; LI-COR). Total intensity values for each fraction, determined by scanning each lane of the Revert stain image, were used to relativize each SusG signal. Relativized OMV and OM SusG fluorescence signals were used to calculate an OMV/OM SusG ratio. Such a ratio was considered 100% for the WT LES SusG construct. Statistical significance between different OMV/OM ratios was determined by an unpaired *t* test for each pair of SusG LES variants.

**Proteinase K assays.** Strains from *B. thetaiotaomicron* were grown in minimal medium with glucose, and cells were washed with phosphate-buffered saline (PBS) and normalized to an optical density at 600 nm (OD$_{600}$) of 9/ml. PBS (540 $\mu$l) and 10 $\mu$l of a proteinase K (ProK) solution (20 mg/ml) were added to 450 $\mu$l of the cell suspension. Tubes were incubated at 37°C, and 200-$\mu$l aliquots were removed at different time points and precipitated using trichloroacetic acid (TCA; final concentration, 20% [vol/wt]). Precipitated aliquots were washed twice with acetone, and pellets were resuspended into Laemmli buffer for Western blot analysis. A nontreated control of the cell suspension was incubated for the longest time point of the experiment and TCA precipitated as described above. A similar procedure was followed for OMV ProK treatments; 450 $\mu$l of purified OMVs was treated under the same conditions as whole cells.

**Growth curves and OMV complementation.** For growth curves, wild-type or $\Delta susG$ strains were grown overnight in TYG medium. Cultures were washed with minimal medium (MM) without any carbon source and normalized by their OD$_{600}$ values. Minimal medium with 0.5% starch as the only carbon source was inoculated with WT or $\Delta susG$ strains to a final OD$_{600}$ of 0.05. OMVs were purified from $\Delta susG$ strains containing different pFD340/*susG*-6×His derivatives grown in minimal medium with glucose and were added to the $\Delta susG$ cultures in minimal medium with starch (1 $\mu$g/ml final OMV concentration). Aliquots were taken at different times, and the OD$_{600}$ was measured to determine growth. Statistical significance when two growth curves were compared was determined by performing one pair of an unpaired *t* test analysis per each time point.

**Transmission electron microscopy.** For negative staining and analysis by transmission electron microscopy, bacterial suspensions in PBS were allowed to absorb onto freshly glow-discharged Formvar/carbon-coated copper grids for 10 min. Grids were washed in distilled H$_2$O and stained with 1% aqueous uranyl acetate (Ted Pella, Inc., Redding, CA) for 1 min. Excess liquid was gently wicked off, and grids were allowed to air dry. Samples were viewed on a JEOL 1200EX transmission electron microscope (JEOL United States, Peabody, MA) equipped with an 8-megapixel digital camera (Advanced Microscopy Techniques, Woburn, MA).

**Data availability.** The mass spectrometry proteomics data have been deposited in the Proteome Xchange Consortium via the PRIDE partner repository with the data set identifier PXD011378 (57).

mSphere®

## SUPPLEMENTAL MATERIAL

Supplemental material for this article may be found at https://doi.org/10.1128/mSphere.00559-18.

**FIG S1,** TIF file, 2.2 MB.
**FIG S2,** TIF file, 1.8 MB.
**FIG S3,** TIF file, 1.5 MB.
**FIG S4,** TIF file, 1 MB.
**TABLE S1,** XLSX file, 2.1 MB.
**TABLE S2,** XLSX file, 0.1 MB.
**TABLE S3,** XLSX file, 0.01 MB.

## REFERENCES

1. Haurat MF, Elhenawy W, Feldman MF. 2015. Prokaryotic membrane vesicles: new insights on biogenesis and biological roles. Biol Chem 396:95–109. https://doi.org/10.1515/hsz-2014-0183.
2. Schwechheimer C, Kuehn MJ. 2015. Outer-membrane vesicles from Gram-negative bacteria: biogenesis and functions. Nat Rev Microbiol 13:605–619. https://doi.org/10.1038/nrmicro3525.
3. Alaniz RC, Deatherage BL, Lara JC, Cookson BT. 2007. Membrane vesicles are immunogenic facsimiles of Salmonella typhimurium that potently activate dendritic cells, prime B and T cell responses, and stimulate protective immunity in vivo. J Immunol 179:7692–7701. https://doi.org/10.4049/jimmunol.179.11.7692.
4. Bomberger JM, Maceachran DP, Coutermarsh BA, Ye S, O'Toole GA, Stanton BA. 2009. Long-distance delivery of bacterial virulence factors by Pseudomonas aeruginosa outer membrane vesicles. PLoS Pathog 5:e1000382. https://doi.org/10.1371/journal.ppat.1000382.
5. Elhenawy W, Debelyy MO, Feldman MF. 2014. Preferential packing of acidic glycosidases and proteases into Bacteroides outer membrane vesicles. mBio 5:e00909–e00914. https://doi.org/10.1128/mBio.00909-14.
6. Ellis TN, Kuehn MJ. 2010. Virulence and immunomodulatory roles of bacterial outer membrane vesicles. Microbiol Mol Biol Rev 74:81–94. https://doi.org/10.1128/MMBR.00031-09.
7. Hickey CA, Kuhn KA, Donermeyer DL, Porter NT, Jin C, Cameron EA, Jung H, Kaiko GE, Wegorzewska M, Malvin NP, Glowacki RW, Hansson GC, Allen PM, Martens EC, Stappenbeck TS. 2015. Colitogenic Bacteroides thetaiotaomicron antigens access host immune cells in a sulfatase-dependent manner via outer membrane vesicles. Cell Host Microbe 17:672–680. https://doi.org/10.1016/j.chom.2015.04.002.
8. Shen Y, Giardino Torchia ML, Lawson GW, Karp CL, Ashwell JD, Mazmanian SK. 2012. Outer membrane vesicles of a human commensal mediate immune regulation and disease protection. Cell Host Microbe 12:509–520. https://doi.org/10.1016/j.chom.2012.08.004.
9. Haurat MF, Aduse-Opoku J, Rangarajan M, Dorobantu L, Gray MR, Curtis MA, Feldman MF. 2011. Selective sorting of cargo proteins into bacterial membrane vesicles. J Biol Chem 286:1269–1276. https://doi.org/10.1074/jbc.M110.185744.
10. Elhenawy W, Bording-Jorgensen M, Valguarnera E, Haurat MF, Wine E, Feldman MF. 2016. LPS remodeling triggers formation of outer membrane vesicles in Salmonella. mBio 7:e00940-16. https://doi.org/10.1128/mBio.00940-16.
11. Bonnington KE, Kuehn MJ. 2016. Outer membrane vesicle production facilitates LPS remodeling and outer membrane maintenance in Salmonella during environmental transitions. mBio 7:e01532-16. https://doi.org/10.1128/mBio.01532-16.
12. Kadurugamuwa JL, Beveridge TJ. 1995. Virulence factors are released from Pseudomonas aeruginosa in association with membrane vesicles during normal growth and exposure to gentamicin: a novel mechanism of enzyme secretion. J Bacteriol 177:3998–4008. https://doi.org/10.1128/jb.177.14.3998-4008.1995.
13. Roier S, Zingl FG, Cakar F, Durakovic S, Kohl P, Eichmann TO, Klug L, Gadermaier B, Weinzerl K, Prassl R, Lass A, Daum G, Reidl J, Feldman MF, Schild S. 2016. A novel mechanism for the biogenesis of outer membrane vesicles in Gram-negative bacteria. Nat Commun 7:10515. https://doi.org/10.1038/ncomms10515.
14. Gilbert JA, Blaser MJ, Caporaso JG, Jansson JK, Lynch SV, Knight R. 2018. Current understanding of the human microbiome. Nat Med 24:392. https://doi.org/10.1038/nm.4517.
15. Lozupone CA, Stombaugh JI, Gordon JI, Jansson JK, Knight R. 2012. Diversity, stability and resilience of the human gut microbiota. Nature 489:220–230. https://doi.org/10.1038/nature11550.
16. Stentz R, Osborne S, Horn N, Li AW, Hautefort I, Bongaerts R, Rouyer M, Bailey P, Shears SB, Hemmings AM, Brearley CA, Carding SR. 2014. A bacterial homolog of a eukaryotic inositol phosphate signaling enzyme mediates cross-kingdom dialog in the mammalian gut. Cell Rep 6:646–656. https://doi.org/10.1016/j.celrep.2014.01.021.
17. Martens EC, Chiang HC, Gordon JI. 2008. Mucosal glycan foraging enhances fitness and transmission of a saccharolytic human gut bacterial symbiont. Cell Host Microbe 4:447–457. https://doi.org/10.1016/j.chom.2008.09.007.
18. Bjursell MK, Martens EC, Gordon JI. 2006. Functional genomic and metabolic studies of the adaptations of a prominent adult human gut symbiont, Bacteroides thetaiotaomicron, to the suckling period. J Biol Chem 281:36269–36279. https://doi.org/10.1074/jbc.M606509200.
19. Martens EC, Lowe EC, Chiang H, Pudlo NA, Wu M, McNulty NP, Abbott DW, Henrissat B, Gilbert HJ, Bolam DN, Gordon JI. 2011. Recognition and degradation of plant cell wall polysaccharides by two human gut symbionts. PLoS Biol 9:e1001221. https://doi.org/10.1371/journal.pbio.1001221.
20. Foley MH, Cockburn DW, Koropatkin NM. 2016. The Sus operon: a model system for starch uptake by the human gut Bacteroidetes. Cell Mol Life Sci 73:2603–2617. https://doi.org/10.1007/s00018-016-2242-x.
21. Schwalm ND, III, Townsend GE, II, Groisman EA. 2016. Multiple signals govern utilization of a polysaccharide in the gut bacterium Bacteroides thetaiotaomicron. mBio 7:e01342-16. https://doi.org/10.1128/mBio.01342-16.
22. Miyazaki K, Hirase T, Kojima Y, Flint HJ. 2005. Medium- to large-sized xylo-oligosaccharides are responsible for xylanase induction in Prevotella bryantii B14. Microbiology 151:4121–4125. https://doi.org/10.1099/mic.0.28270-0.
23. Sonnenburg ED, Zheng H, Joglekar P, Higginbottom S, Firbank SJ, Bolam DN, Sonnenburg JL. 2010. Specificity of polysaccharide use in intestinal

Bacteroides species determines diet-induced microbiota alterations. Cell 141:1241–1252. https://doi.org/10.1016/j.cell.2010.05.005.

24. Sonnenburg JL, Xu J, Leip DD, Chen CH, Westover BP, Weatherford J, Buhler JD, Gordon JI. 2005. Glycan foraging in vivo by an intestine-adapted bacterial symbiont. Science 307:1955–1959. https://doi.org/10.1126/science.1109051.

25. Rakoff-Nahoum S, Coyne MJ, Comstock LE. 2014. An ecological network of polysaccharide utilization among human intestinal symbionts. Curr Biol 24:40–49. https://doi.org/10.1016/j.cub.2013.10.077.

26. Rakoff-Nahoum S, Foster KR, Comstock LE. 2016. The evolution of co-operation within the gut microbiota. Nature 533:255–259. https://doi.org/10.1038/nature17626.

27. Shipman JA, Berleman JE, Salyers AA. 2000. Characterization of four outer membrane proteins involved in binding starch to the cell surface of Bacteroides thetaiotaomicron. J Bacteriol 182:5365–5372. https://doi.org/10.1128/JB.182.19.5365-5372.2000.

28. Glenwright AJ, Pothula KR, Bhamidimarri SP, Chorev DS, Basle A, Firbank SJ, Zheng H, Robinson CV, Winterhalter M, Kleinekathofer U, Bolam DN, van den Berg B. 2017. Structural basis for nutrient acquisition by dominant members of the human gut microbiota. Nature 541:407–411. https://doi.org/10.1038/nature20828.

29. Wilson MM, Anderson DE, Bernstein HD. 2015. Analysis of the outer membrane proteome and secretome of Bacteroides fragilis reveals a multiplicity of secretion mechanisms. PLoS One 10:e0117732. https://doi.org/10.1371/journal.pone.0117732.

30. Ottman N, Huuskonen L, Reunanen J, Boeren S, Klievink J, Smidt H, Belzer C, de Vos WM. 2016. Characterization of outer membrane proteome of Akkermansia muciniphila reveals sets of novel proteins exposed to the human intestine. Front Microbiol 7:1157. https://doi.org/10.3389/fmicb.2016.01157.

31. Renzi F, Manfredi P, Mally M, Moes S, Jenö P, Cornelis GR. 2011. The N-glycan glycoprotein deglycosylation complex (Gpd) from Capnocytophaga canimorsus deglycosylates human IgG. PLoS Pathog 7:e1002118. https://doi.org/10.1371/journal.ppat.1002118.

32. Lauber F, Cornelis GR, Renzi F. 2016. Identification of a new lipoprotein export signal in Gram-negative bacteria. mBio 7:e01232-16. https://doi.org/10.1128/mBio.01232-16.

33. Shipman JA, Cho KH, Siegel HA, Salyers AA. 1999. Physiological characterization of SusG, an outer membrane protein essential for starch utilization by Bacteroides thetaiotaomicron. J Bacteriol 181:7206–7211.

34. Koropatkin NM, Smith TJ. 2010. SusG: a unique cell-membrane-associated alpha-amylase from a prominent human gut symbiont targets complex starch molecules. Structure 18:200–215. https://doi.org/10.1016/j.str.2009.12.010.

35. Spence C, Wells WG, Smith CJ. 2006. Characterization of the primary starch utilization operon in the obligate anaerobe Bacteroides fragilis: regulation by carbon source and oxygen. J Bacteriol 188:4663–4672. https://doi.org/10.1128/JB.00125-06.

36. Luis AS, Briggs J, Zhang X, Farnell B, Ndeh D, Labourel A, Basle A, Cartmell A, Terrapon N, Stott K, Lowe EC, McLean R, Shearer K, Schuckel J, Venditto I, Ralet MC, Henrissat B, Martens EC, Mosimann SC, Abbott DW, Gilbert HJ. 2018. Dietary pectic glycans are degraded by coordinated enzyme pathways in human colonic Bacteroides. Nat Microbiol 3:210–219. https://doi.org/10.1038/s41564-017-0079-1.

37. Cameron EA, Kwiatkowski KJ, Lee BH, Hamaker BR, Koropatkin NM, Martens EC. 2014. Multifunctional nutrient-binding proteins adapt human symbiotic bacteria for glycan competition in the gut by separately promoting enhanced sensing and catalysis. mBio 5:e01441-14. https://doi.org/10.1128/mBio.01441-14.

38. Hooda Y, Shin HE, Bateman TJ, Moraes TF. 2017. Neisserial surface lipoproteins: structure, function and biogenesis. Pathog Dis 75:ftx010.

39. Konovalova A, Perlman DH, Cowles CE, Silhavy TJ. 2014. Transmembrane domain of surface-exposed outer membrane lipoprotein RcsF is threaded through the lumen of beta-barrel proteins. Proc Natl Acad Sci U S A 111:E4350–E4358. https://doi.org/10.1073/pnas.1417138111.

40. Konovalova A, Silhavy TJ. 2015. Outer membrane lipoprotein biogenesis: Lol is not the end. Philos Trans R Soc B Biol Sci 370:20150030. https://doi.org/10.1098/rstb.2015.0030.

41. Hooda Y, Moraes TF. 2018. Translocation of lipoproteins to the surface of gram negative bacteria. Curr Opin Struct Biol 51:73–79. https://doi.org/10.1016/j.sbi.2018.03.006.

42. Hooda Y, Lai CC, Judd A, Buckwalter CM, Shin HE, Gray-Owen SD, Moraes TF. 2016. Slam is an outer membrane protein that is required for the surface display of lipidated virulence factors in Neisseria. Nat Microbiol 1:16009. https://doi.org/10.1038/nmicrobiol.2016.9.

43. Stahl M, Friis LM, Nothaft H, Liu X, Li J, Szymanski CM, Stintzi A. 2011. L-Fucose utilization provides Campylobacter jejuni with a competitive advantage. Proc Natl Acad Sci U S A 108:7194–7199. https://doi.org/10.1073/pnas.1014125108.

44. Ng KM, Ferreyra JA, Higginbottom SK, Lynch JB, Kashyap PC, Gopinath S, Naidu N, Choudhury B, Weimer BC, Monack DM, Sonnenburg JL. 2013. Microbiota-liberated host sugars facilitate post-antibiotic expansion of enteric pathogens. Nature 502:96–99. https://doi.org/10.1038/nature12503.

45. Bacic MK, Smith CJ. 2008. Laboratory maintenance and cultivation of bacteroides species. Curr Protoc Microbiol Chapter 13:Unit 13C 1.

46. Smith CJ, Rogers MB, McKee ML. 1992. Heterologous gene expression in Bacteroides fragilis. Plasmid 27:141–154. https://doi.org/10.1016/0147-619X(92)90014-2.

47. Koropatkin NM, Martens EC, Gordon JI, Smith TJ. 2008. Starch catabolism by a prominent human gut symbiont is directed by the recognition of amylose helices. Structure 16:1105–1115. https://doi.org/10.1016/j.str.2008.03.017.

48. Scott NE, Parker BL, Connolly AM, Paulech J, Edwards AV, Crossett B, Falconer L, Kolarich D, Djordjevic SP, Hojrup P, Packer NH, Larsen MR, Cordwell SJ. 2011. Simultaneous glycan-peptide characterization using hydrophilic interaction chromatography and parallel fragmentation by CID, higher energy collisional dissociation, and electron transfer dissociation MS applied to the N-linked glycoproteome of Campylobacter jejuni. Mol Cell Proteomics 10:M000031MCP201. https://doi.org/10.1074/mcp.M000031-MCP201.

49. Ishihama Y, Rappsilber J, Mann M. 2006. Modular stop and go extraction tips with stacked disks for parallel and multidimensional peptide fractionation in proteomics. J Proteome Res 5:988–994. https://doi.org/10.1021/pr050385q.

50. Rappsilber J, Mann M, Ishihama Y. 2007. Protocol for micro-purification, enrichment, pre-fractionation and storage of peptides for proteomics using StageTips. Nat Protoc 2:1896–1906. https://doi.org/10.1038/nprot.2007.261.

51. Cox J, Mann M. 2008. MaxQuant enables high peptide identification rates, individualized p.p.b.-range mass accuracies and proteome-wide protein quantification. Nat Biotechnol 26:1367–1372. https://doi.org/10.1038/nbt.1511.

52. Cox J, Hein MY, Luber CA, Paron I, Nagaraj N, Mann M. 2014. Accurate proteome-wide label-free quantification by delayed normalization and maximal peptide ratio extraction, termed MaxLFQ. Mol Cell Proteomics 13:2513–2526. https://doi.org/10.1074/mcp.M113.031591.

53. Tyanova S, Temu T, Carlson A, Sinitcyn P, Mann M, Cox J. 2015. Visualization of LC-MS/MS proteomics data in MaxQuant. Proteomics 15:1453–1456. https://doi.org/10.1002/pmic.201400449.

54. Tsirigos KD, Peters C, Shu N, Kall L, Elofsson A. 2015. The TOPCONS web server for consensus prediction of membrane protein topology and signal peptides. Nucleic Acids Res 43:W401–W407. https://doi.org/10.1093/nar/gkv485.

55. Juncker AS, Willenbrock H, Von Heijne G, Brunak S, Nielsen H, Krogh A. 2003. Prediction of lipoprotein signal peptides in Gram-negative bacteria. Protein Sci 12:1652–1662. https://doi.org/10.1110/ps.0303703.

56. Crooks GE, Hon G, Chandonia JM, Brenner SE. 2004. WebLogo: a sequence logo generator. Genome Res 14:1188–1190. https://doi.org/10.1101/gr.849004.

57. Vizcaíno JA, Csordas A, del-Toro N, Dianes JA, Griss J, Lavidas I, Mayer G, Perez-Riverol Y, Reisinger F, Ternent T, Xu QW, Wang R, Hermjakob H. 2016. 2016 update of the PRIDE database and related tools. Nucleic Acids Res 44:D447–D456. https://doi.org/10.1093/nar/gkv1145.